ARMY RESEARCH LABORATORY

Stochastic Analysis of Initial Extended Area Protection and Survivability (EAPS) Projectile

by Michael M. Chen

ARL-TR-4140 **June 2007**

NOTICES

Disclaimers

The findings in this report are not to be construed as an official Department of the Army position unless so designated by other authorized documents.

Citation of manufacturer's or trade names does not constitute an official endorsement or approval of the use thereof.

DESTRUCTION NOTICE—Destroy this report when it is no longer needed. Do not return it to the originator.

Army Research Laboratory
Aberdeen Proving Ground, MD 21005-5066

ARL-TR-4140 **June 2007**

Stochastic Analysis of Initial Extended Area Protection and Survivability (EAPS) Projectile

Michael M. Chen
Weapons and Materials Research Directorate, ARL

REPORT DOCUMENTATION PAGE

Form Approved
OMB No. 0704-0188

1. REPORT DATE *(DD-MM-YYYY)*	2. REPORT TYPE	3. DATES COVERED (From - To)
June 2007	Final	October 2006 through April 2007

4. TITLE AND SUBTITLE

Stochastic Analysis of Initial Extended Area Protection and Survivability (EAPS) Projectile

5a. CONTRACT NUMBER

5b. GRANT NUMBER

5c. PROGRAM ELEMENT NUMBER

6. AUTHOR(S)

Michael M. Chen (ARL)

5d. PROJECT NUMBER

622618.H80

5e. TASK NUMBER

5f. WORK UNIT NUMBER

7. PERFORMING ORGANIZATION NAME(S) AND ADDRESS(ES)

U.S. Army Research Laboratory
Weapons and Materials Research Directorate
Aberdeen Proving Ground, MD 21005-5066

8. PERFORMING ORGANIZATION REPORT NUMBER

ARL-TR-4140

9. SPONSORING/MONITORING AGENCY NAME(S) AND ADDRESS(ES)

10. SPONSOR/MONITOR'S ACRONYM(S)

11. SPONSOR/MONITOR'S REPORT NUMBER(S)

12. DISTRIBUTION/AVAILABILITY STATEMENT

Approved for public release; distribution is unlimited.

13. SUPPLEMENTARY NOTES

14. ABSTRACT

Gun propulsion modeling has been undergoing development for many decades. Because of the great strides in recent development, one has been able to estimate in-bore pressure-time history at a fairly accurate level. However, some underlying assumptions among the models exhibit certain level of uncertainties, such as the time-varying friction between the obturator and bore surface, the granular shape variations of propelling charges, the packaging deviations of each propellant load, etc. These factors explain the fact that the recorded pressure levels differ from one gun shot to another with the same gun and projectile system in many experimental tests. Thus, this report considered the variations of the factors as a whole and investigated in-bore responses of the Extended Area Protection and Survivability projectile, subject to the inherent randomness of propulsion forces. The results provide a better understanding of the projectile behavior during proposed circumstances.

15. SUBJECT TERMS

base pressure variations; EAPS projectile; Monte Carlo simulation; stochastic analysis

16. SECURITY CLASSIFICATION OF:			17. LIMITATION OF ABSTRACT	18. NUMBER OF PAGES	19a. NAME OF RESPONSIBLE PERSON
a. REPORT	b. ABSTRACT	c. THIS PAGE			Michael M. Chen
Unclassified	Unclassified	Unclassified	SAR	30	19b. TELEPHONE NUMBER (*Include area code*) 410-278-6146

Contents

List of Figures

List of Tables

Acknowledgments

The author would like to thank

Dr. Lang-Mann Chang, a retiree from the Propulsion Science Branch of the U.S. Army Research Laboratory (ARL), for his valuable advice about the physics of gun propellant combustion.

Dr. Peter Plostins, ARL program manager of the EAPS project, for providing financial support for this study.

This work was supported in part by a grant of high-performance computing time from the U.S. Department of Defense High Performance Computing Modernization program at ARL's Major Shared Resource Center, Aberdeen Proving Ground, Maryland.

INTENTIONALLY LEFT BLANK

1. Introduction

A mission program named Extended Area Protection and Survivability (EAPS) was initiated by the U.S. Army Aviation and Missile Research Development and Engineering Center (AMRDEC). The objective of the mission is to develop guided ammunition technologies to defend the battle space against any presented targets. Specifically, critical supporting technologies, including interceptor, sensor, and fire controls, which can enable stationary and mobile 360-degree hemispherical extended area protection from direct and indirect fires, would be demonstrated through this program. The EAPS projectile system is intended to hit and destroy hostile objects, such as mortars, rockets, and artillery. With the constraint of short reaction time, flight stability and trajectory accuracy have become critical concerns for the mission of interception. In fact, the overall projectile performance may be affected by a variety of factors at any stage of the launch process, starting from primer ignition, propellant combustion, projectile in-bore travel, and free-body flight throughout target hitting. To support the mission, preliminary structural design and analysis of an initial EAPS projectile system has been performed by Chen (*1, 2*) to ensure that the structural integrity is maintained during launch. In addition, the responses of the EAPS projectile, subject to gun barrel centerline variations, including transitional and rotational velocities at the muzzle, have been investigated (*3*). The focus of this report is to gain some insight into the phenomenon that no repeatable pressure-time curves were obtained through experimental tests, even with the same kind of the projectile and ammunition system. It explains that some level of variations exists in the generation process of propulsion forces, which may affect in-bore projectile behavior. The uncertainty should be studied and taken into account when one is designing a highly reliable weapon system such as EAPS ammunition system.

The modeling of complex gun propulsion schemes has evolved at a great stride over the past two decades. In the mid-1980s, a lumped parameter computer code IBHVG2 (Interior Ballistics of High Velocity Gun, version 2), developed by the U.S. Army Research Laboratory[1] (ARL), was available for the calculation of interior ballistic trajectories, including time-dependent gas pressure, projectile displacement and velocity (*4*). In the early 1990s, the efforts were extended to one-dimensional and two-dimensional interior ballistic modeling, where a number of experimental studies have demonstrated space-time-dependent flame spreading processes (*5, 6*). Over the past decade, more details in determining gun distributed pressure field have been taken into account for chamber pressure calculations, particularly in the ignition phase. The additional consideration had led to the development of next generation model named NGEN (*7*). The NGEN codes are three-dimensional (3-D), multiphase, and computational fluid dynamics-based computer program and have been used for a number of applications in recent years (*8, 9*). At present, an in-bore pressure-time curve can be estimated at a fairly accurate level.

[1]At that time, the U.S. Army Ballistics Research Laboratory.

Nevertheless, a few factors that are inherently uncontrollable and exhibit a certain level of variations exist when in-bore pressure history is calculated. Examples, such as time-varying frictions between obturator and bore surface, gun barrel manufacturing tolerance, granular shape variations of propelling charges, packaging deviations of each propellant load, distinctive flame spreading path, changing ambient temperature, etc., may contribute to the variations. In reality, the pressure records from many experimental shootings at Aberdeen Proving Ground, Maryland, have demonstrated the deviations. The differences from one shot to another could be attributed to one or more of the prescribed factors. Understandably, the pressure deviations would become more obvious at a war field because of additional weather and environmental issues. Thus, it is important to study how the performance of the EAPS projectile is influenced by the stochastic excitations derived from the combustion of propellants. The objective of this report was not to model the random nature of each factor individually. Instead, the variations of all the contributing factors were considered as a whole. A pressure-time curve, where the pressure level at each time step was modeled as a Gaussian variable, was adopted for this study.

2. Description of the EAPS Projectile System

The initial EAPS projectile was equipped with a windscreen and a penetrator in the front, which has an ogive length and radius of 70.5 mm and 1380 mm, respectively. Four fins for stabilization had a fin span of 50 mm. The length of the projectile from nose to tail was 317 mm. An outer diameter of 23.5 mm was used for this study. The inside of the projectile body was divided into two cavity areas. The forward cavity may carry high explosive payload while the rear cavity was designed to accommodate electronic equipment. Figure 1 shows the 3-D geometry model of the EAPS projectile. In general, the launch package consisted of projectile body, penetrator, windscreen, electronics, fins, and sabot. The material configuration from a cross-sectional view of the projectile system is illustrated in figure 2. The sabot and windscreen cover were composed of 7075-T651 aluminum alloy. Tungsten material was used for the penetrator. The gun barrel, projectile body and fins were modeled with 17-4 PH[2] stainless steel. The detailed physical and mechanical properties of the material for each component are presented in a previous report (*1*).

A 64-caliber smooth bore gun tube with an inner diameter of 60 mm was used to simulate the projectile firing. The barrel has a total length of 3840 mm, i.e., in-bore travel distance for the projectile. M2 propellants with a geometry of seven perforation grains were used for the propulsion. Given a chamber volume of 1.3 liters, a peak breech pressure of 470 MPa was derived from IBHVG2. For computational efficiency in a stochastic study, the windscreen and stabilized fins were substituted with equivalent weight so that the center of gravity of the projectile system remained at the same location. The simplification avoided very fine mesh and significantly

[2] 17-4 PH is a registered trademark of AK Steel Corporation.

reduced computational time. In addition, the weight of the sabot component was optimized, which reduced the total mass of the launch system to approximately 1 kg. The simplified projectile configuration and grids are displayed in figure 3. This finite element model contained eight-node solid hexahedral elements. Note that no tolerance in the diameter of the bore-riders was modeled for the statistical simulation. Surface-to-surface contact elements were used for the interface with the gun barrel.

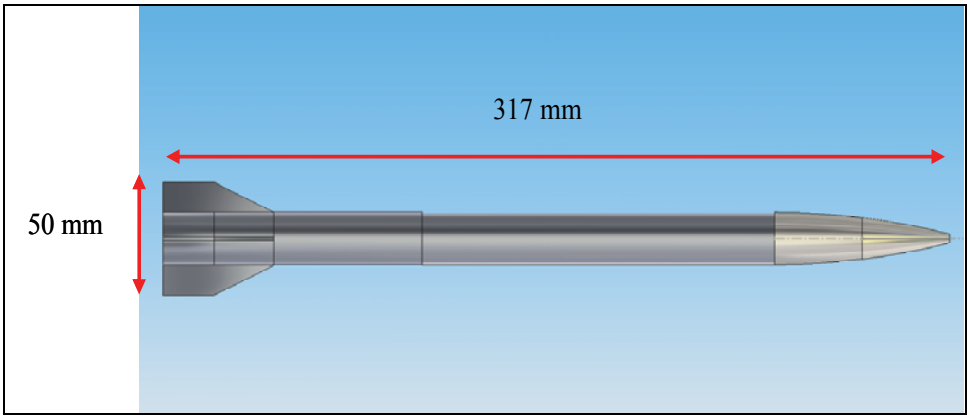

Figure 1. Geometry of the initial EAPS projectile.

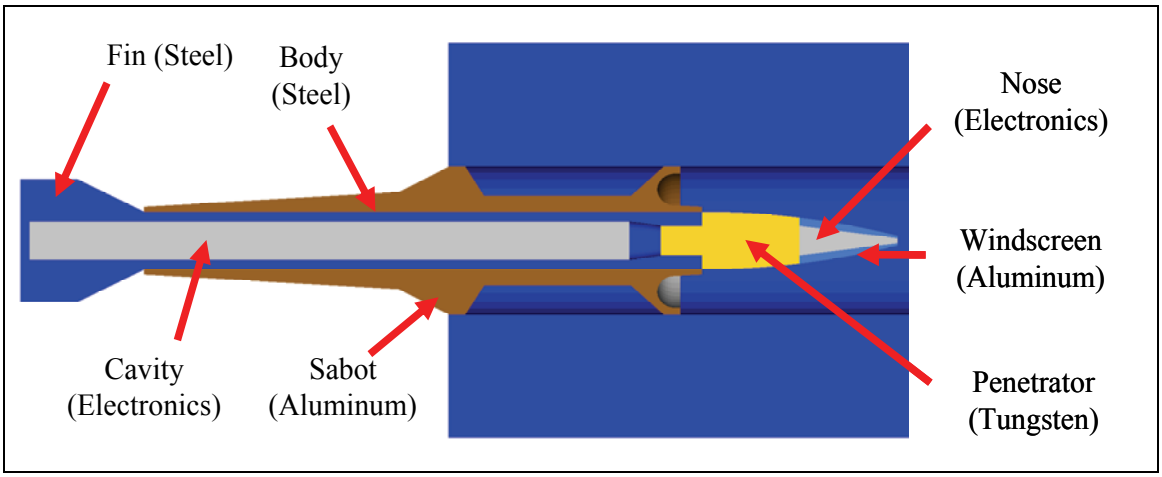

Figure 2. Material configuration of the initial EAPS projectile.

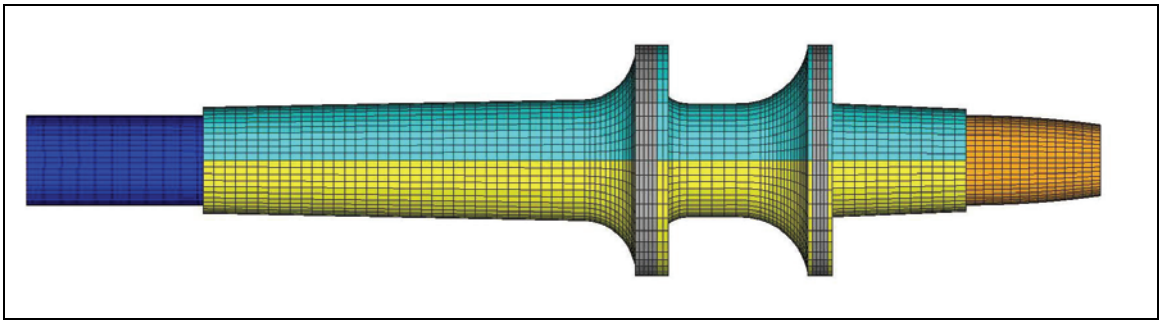

Figure 3. Simplified configuration of the initial EAPS finite element model.

3. Stochastic Modeling

A base pressure-time curve shown in figure 4 was adopted for the study. A peak pressure of 315 MPa occurred at 2 ms from ignition, and the total pressure duration was 4.7 ms. Given the random nature of pressure generation through the propellant burning process, the pressure level at each time step was considered as a normally distributed function. As a result, 47 Gaussian variables were created to represent the profile of the stochastic process. This modeling may account for the fact that the measured pressure level of every experimental shot differed, even with the same gun, the same cartridge and the same projectile. The normal distribution can be expressed as

$$f(x) = \frac{1}{\sqrt{2\pi\sigma^2}} e^{-\frac{(x-\mu)^2}{2\sigma^2}}$$

in which μ is the mean and σ is the standard deviation. Because the pressure differentiation among experimental firings was not substantial, a coefficient of variation (COV) of 3% from the mean pressure of the time step for the random variables was adopted (*10*). Note that no additional energy was imposed on the projectile system as opposed to the pressure curve since the ensemble mean remained the same.

To better illustrate the pressure deviations, figure 5 shows the Gaussian distributions of the base pressures at the time steps of 1.8, 1.9, and 2.0 ms from ignition. It is a locally magnified view in the corresponding time steps of figure 4. The middle line with square points represents the mean value of the pressure, and the lines above and below with triangular points stand for one standard deviation from the mean. The bell shapes depict the spread of the random variables. In other words, the pressure at each time step is most likely to take place. The likelihood of occurrence gradually decreases for the pressure values away from the pressure. This report adopted Monte Carlo simulation technique to randomly generate a total number of 100 samples on the basis of Gaussian distribution properties. As a result, 100 simulated cases, each with a distinctive pressure-time curve, were constituted. The detail of Monte Carlo simulated base pressures is provided in appendix A. The pressure curves for the first three cases are shown in figure 6. Because of low values in the initial stage, the variations are not visible because of the scale. The uncommon small double bumps in high pressure area have to be achieved with complex configurations of propelling charges or a certain combination of multi-physical scenario, which is beyond the scope of the report.

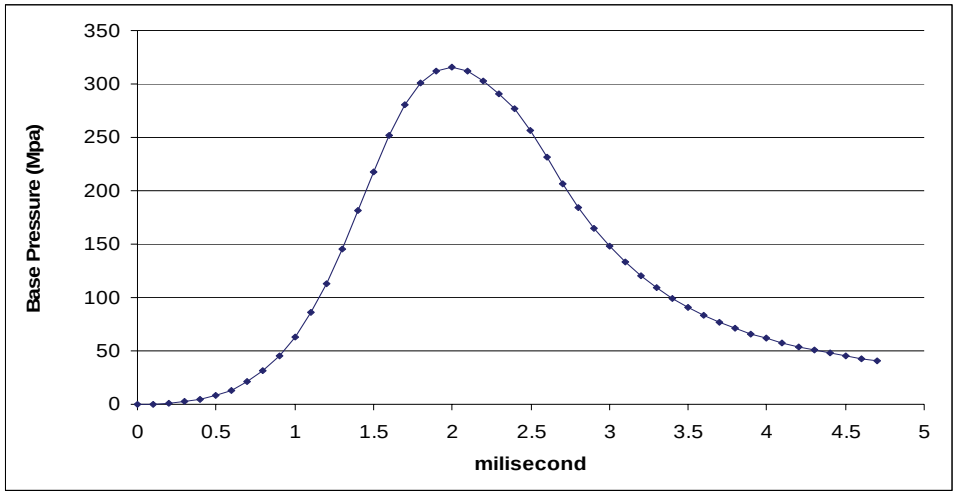

Figure 4. A pressure-time curve at the base of the EAPS projectile.

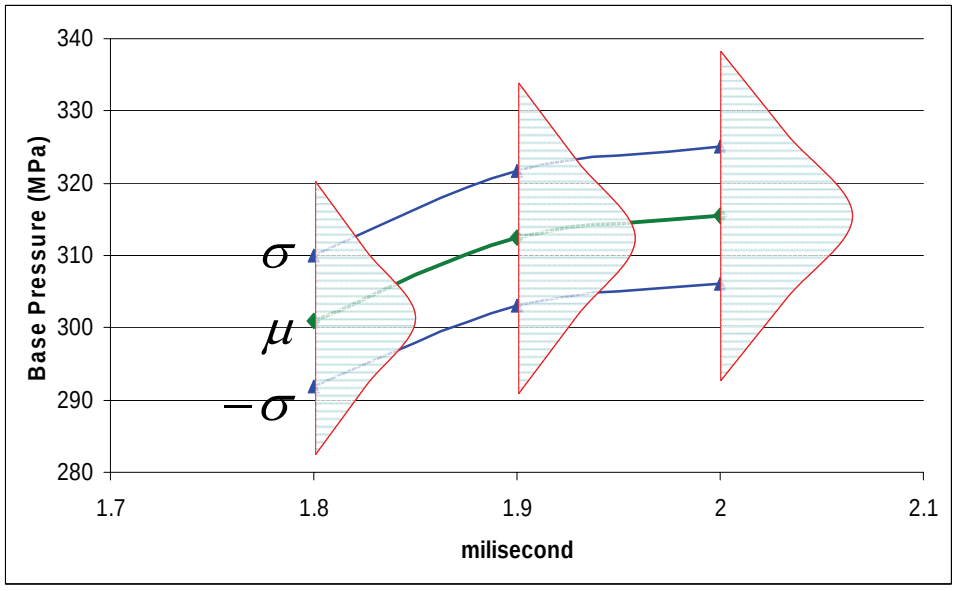

Figure 5. Gaussian distributions (shaded areas) of the base pressures at the time steps of 1.8, 1.9, and 2.0 ms from ignition.

It is necessary to evaluate if the 100 samples are sufficient to represent a Gaussian distribution. Figure 7 gives a histogram plot for the random variable 20, i.e., the peak pressure at 2.0 ms travel time from ignition. The monotonic line on the chart represents cumulative distribution function (cdf), and the other curve shown stands for probability density function (pdf). The histogram passed a normality test at 95% confidence level although a little right skewed is seen on the chart. In addition, the computed sample average was close to the ensemble average of 315 MPa. It indicates that the sample distribution constituted a good representation of the population profile, i.e., the number of sampling sufficed. Subsequently, explicit dynamic analysis was solved with the

LS-DYNA[3] software, each with a distinct pressure-time sample, on the Linux Networx Evolocity II cluster at ARL's High Performance Computing Center. Each analysis required approximately 2 hours of central processing unit time on eight-thread parallel execution. In summary, the gun-projectile system was subjected to the described stochastic excitations. The system responses would be stochastic even with a deterministic projectile system.

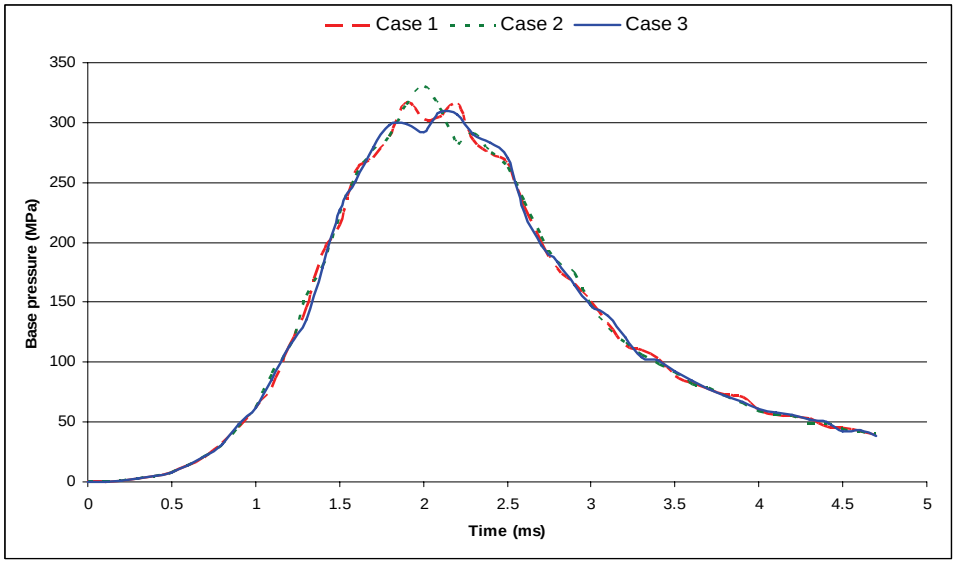

Figure 6. Pressure curves of the first three simulated cases.

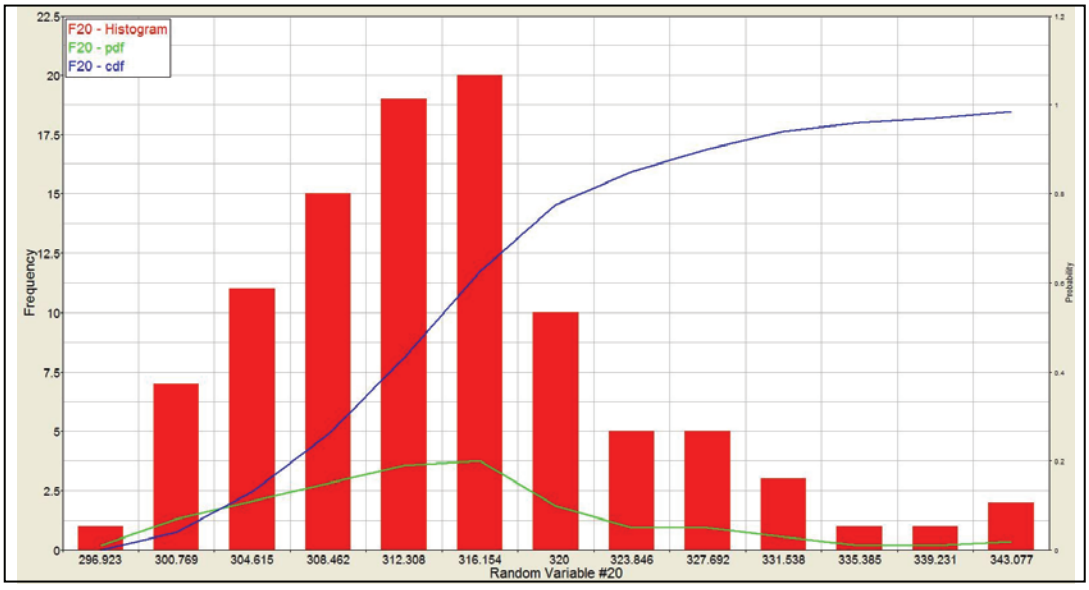

Figure 7. Histogram of random variable 20, i.e., peak pressure distribution.

[3]LS-DYNA, which is not an acronym, is a trademark of Livermore Software Technology Corporation.

4. Stochastic Responses

The dispersions of in-bore projectile responses attributable to the simulated base pressure deviations are of interest. The exit velocity, peak acceleration, maximum von Mises stress, and projectile travel distance were retrieved. The spread of the values may shed some light on what variations and ranges of the projectile responses should be expected even in a normal circumstance of firing. In addition, the derived in-bore response statistics are important for the design of the projectile system and may be further used for the analysis of exterior ballistics and terminal effect evaluations.

Figure 8 depicts a histogram of the axial velocity of the projectile at the muzzle. The mean and standard deviation of the axial velocity were found to be approximately 1551 m/sec and 12.4 m/sec, respectively. Because of a very low COV of 0.8% for the response, most computed data were centralized at the mean. Given the assumption of Gaussian response, which is acceptable in this case, there was a 99.7% likelihood that the axial velocity responses would fall into the range between 1514 m/sec and 1588 m/sec, i.e., within three standard deviations of the mean. The statistics of the projectile axial velocity at the exit were also derived in response to reasonable gun barrel centerline variations in a previous report (*3*). Expectedly, the mean velocity response was in good agreement from both cases since the variations of propulsion forces and barrel centerline were generated and centralized to equivalent values. However, in comparison of the standard deviation of the axial velocity, i.e., 12.4 m/sec versus 8.7 m/sec, the reasonable deviation of applied base pressure appeared to make a greater contribution to the scatter of projectile velocity at the exit as opposed to the reasonable manufacturing tolerance of barrel centerline. The displacement histogram at node 34204, i.e., at the center of the projectile nose, was also obtained and is displayed in figure 9. Because of the number of bins used in the histogram, the distribution shows somewhat non-Gaussian. However, the travel distance data passed a normality test at a 90% confidence level.

In addition, the sampling distribution of the acceleration responses is given in figure 10. The responses at the time of 2.0 ms from ignition, when the peak acceleration occurred corresponding to the pressure-time curve, were collected. The mean value of the acceleration response was computed to be approximately 85,000 g. Unlike velocity, the acceleration distribution exhibits a high spread. One of the major reasons was because of inconsistent occurrence time, namely, the peak accelerations took place at the time step when the peak pressures occurred. One can see the time distinction for the peak values of the pressure curves, as demonstrated in figure 6. As a result, the peak accelerations appeared to be a non-Gaussian distribution. Similarly, figure 11 shows the histogram of von Mises stress response at element 12191 of the projectile body, where the maximum stress occurred corresponding to the pressure-time excitation. The distribution of the von Mises stress at the node exhibited a mean value of 952 MPa. As expected, a wide range and a non-Gaussian distribution of the responses from 894 MPa to 1020 MPa were derived. The intention of

this report was to compare the responses to the simulated pressures with those to the pressure at the same time step, i.e., 2.0 ms from ignition and at the same location, i.e., element 12191. For a more comprehensive comparison, the peak accelerations over the in-bore travel period and the maximum von Mises stress at any element of the entire model should be collected and used from every analysis.

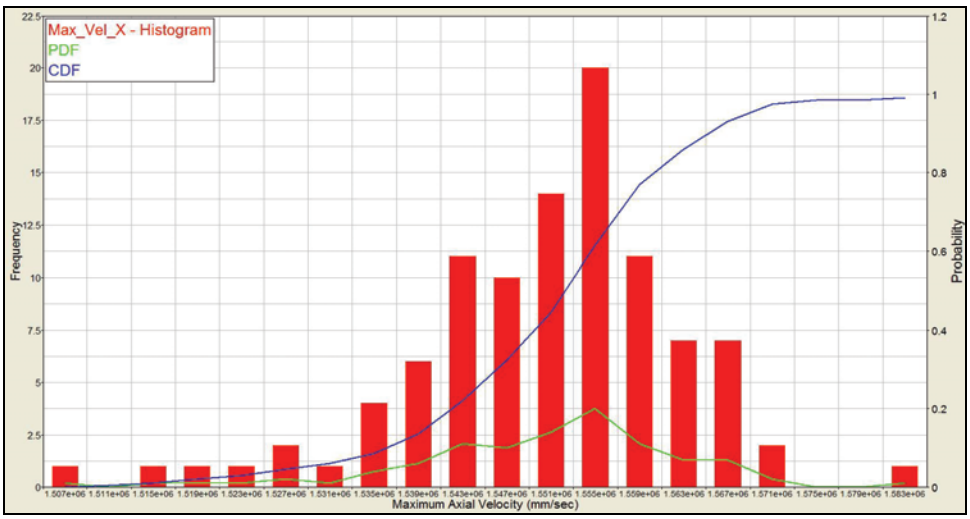

Figure 8. Histogram of maximum axial velocity distribution.

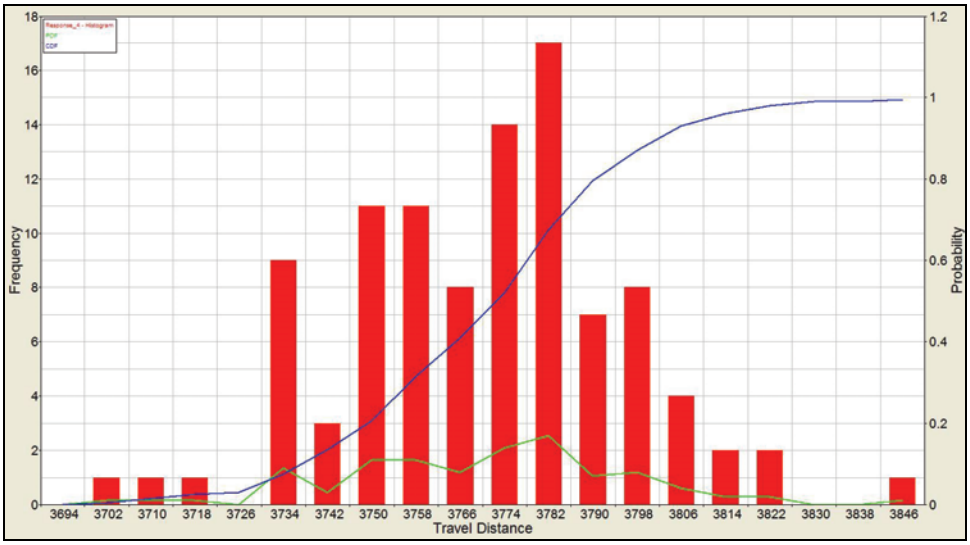

Figure 9. Histogram of total travel distance (mm).

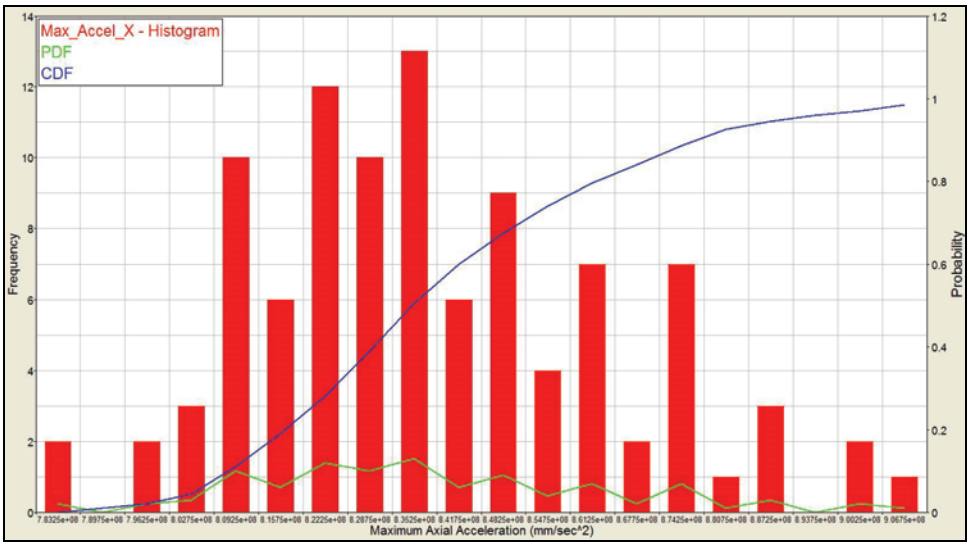

Figure 10. Histogram of axial accelerations at time 2.0 ms from ignition.

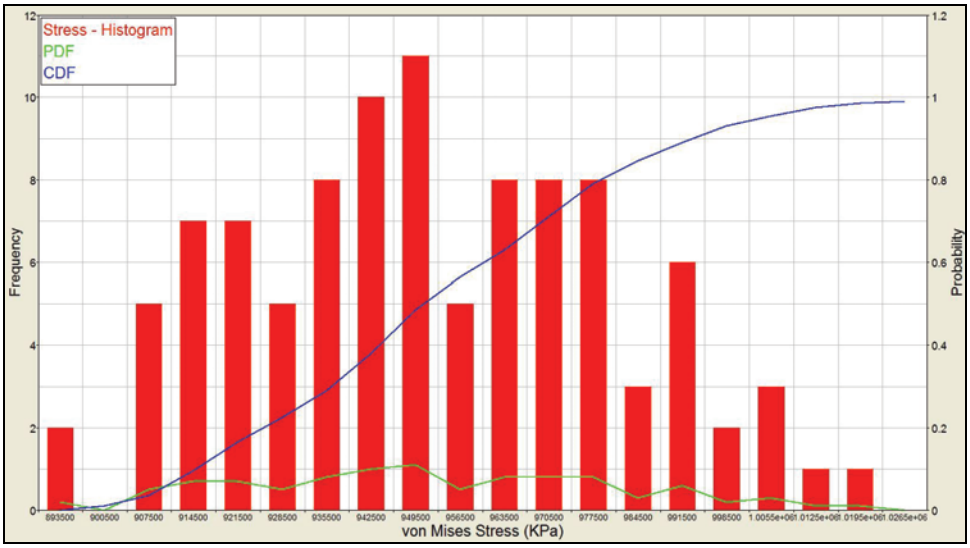

Figure 11. Histogram of von Mises stress at element 12191 of EAPS projectile body.

Response statistics of the projectile including the mean, COV, minimum and maximum values are summarized in table 1. Note that the acceleration and stress responses show COVs of 3.1% and 3.0%, respectively. These second order derivatives exhibited an equivalent COV level compared with that of the applied base pressures. The mean value of the von Mises stress response was computed to be 952 MPa, which was below the yield strength of the 17-4 PH stainless steel material. However, the stress level could rise to 1020 MPa, based on the simulated pressures in this study or to 1038 MPa, based on three-standard-deviation range, given the assumption of normally distributed responses. This implies the possibility of exceeding the strength capacity. Thus, care should be taken when one is designing the projectile material and is considering inherently random pressures. The displacement response at the nose of the projectile demonstrates a

COV of 0.67%—a much smaller variation as anticipated. The mean value of the travel distance was 3770 mm with a standard deviation of 25.3 mm. It indicates that the time duration of the pressure curve should have been a little longer than 4.7 ms for the projectile to reach the muzzle. Based on the simulated results, the likelihood to travel through the barrel within the time frame was less than 10%. The discrepancy was because of the slight difference in the total mass of the launch package used in computer modeling and IBHVG2.

Table 1. Response statistics of EAPS projectile subject to random excitations.

Response	Mean	Coefficient of Variation (percent)	Minimum	Maximum
Peak velocity (mm/sec)	1.55×10^{6}	0.80	1.506×10^{6}	1.583×10^{6}
Peak acceleration (mm/sec^2)	8.38×10^{8}	3.1	7.80×10^{8}	9.09×10^{8}
von Mises stress at projectile body (KPa)	9.52×10^{5}	3.0	8.94×10^{5}	1.02×10^{6}
Travel Distance (mm)	3770	0.67	3699	3847

The cross-relationships among these responses were evaluated as well in this study. Figure 12 shows the scatter plot of the peak acceleration against the von Mises stress responses. Overall, a positive trend can be seen from the plot. However, the level of correlation was not considerably high because the locations where the nodal acceleration and the element stress were obtained were not identical. In other words, the accelerations were collected at the center of the projectile nose while the stresses were obtained at an element of the projectile body between bulkhead and bore-rider. Another scatter plot that represents the relationships between the maximum axial velocity and the travel distance is given in figure 13. The data demonstrated a very strong correlation as expected. The relationships should help derive required muzzle velocity given a certain length of gun barrel. The scatter plots between the random variables and the responses make little sense because the 47 random variables were not completely independent in terms of their contributions to the total responses. No clear pattern was found between any instant pressure variable and any of the projectile responses.

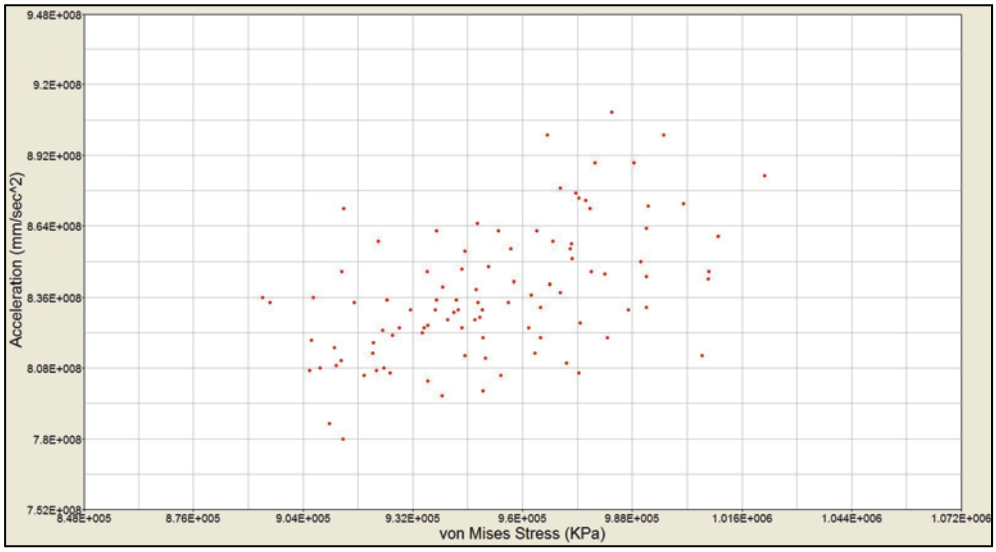

Figure 12. Scatter plot of von Mises stress versus maximum acceleration.

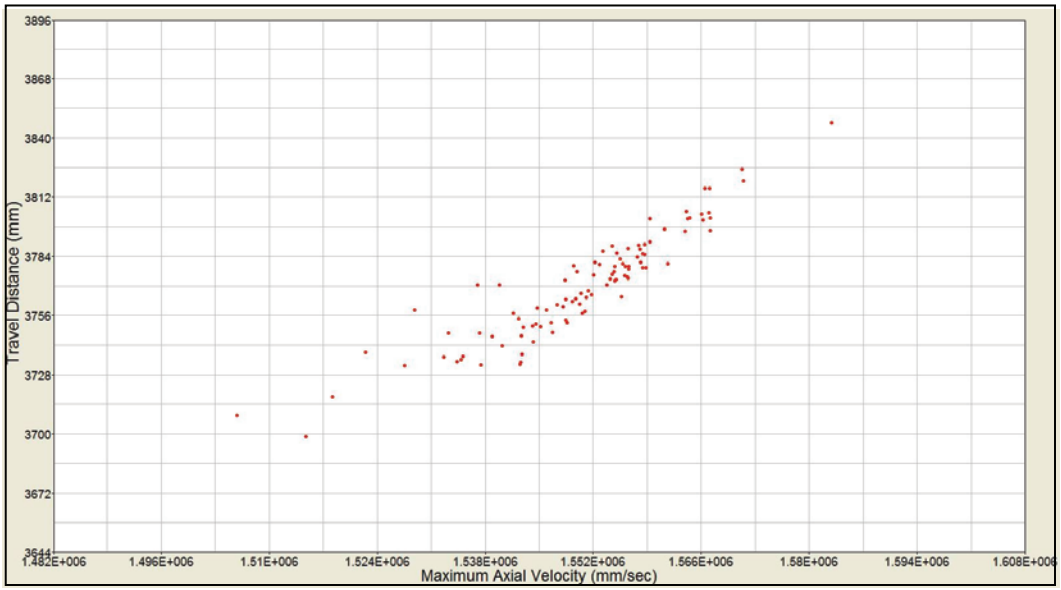

Figure 13. Scatter plot of von Mises stress versus maximum acceleration.

5. Summary

A pressure-time curve that was applied to the base of the EAPS projectile was adopted for the stochastic study. The curve that had a time step of 0.1 ms and an excitation period of 4.7 ms consisted of a total of 47 data points. The pressure level at each data point was considered as a normally distributed random variable. The variations of the pressure were used to account for the uncertainties from a number of inherently uncontrollable factors that are associated with propulsion thrust generation, such as time-varying bore resistance, gun barrel manufacturing tolerance, granular shape variations of propelling charges, packaging deviations of each propellant load, distinctive flame spreading path, and changing ambient temperature. A reasonable 3% COV for each random variable was employed to explain these factors as a whole and to support the evidence that the dispersion of in-bore projectile responses exists in daily experimental shooting even with the same gun, the same cartridge, and the same projectile system. A total of 100 distinctive pressure samples was generated on the basis of 47 Gaussian variables through Monte Carlo simulation techniques. The pressure samples were then applied to a deterministic structural and material model of the EAPS projectile system. Stochastic analysis of the system was conducted and the corresponding in-bore projectile responses to each pressure sample were obtained and analyzed.

It was found that the derived accelerations and von Mises stresses had an equivalent level of COV as opposed to the applied base pressures. The widespread and non-Gaussian distributions of the responses demonstrated that the pressure variations significantly influence the acceleration and

stress responses. On the other hand, the in-bore travel distance and exit velocity were strongly correlated as expected, and both responses exhibited the property of Gaussian distributions. A simplistic estimation may be made if all the responses are assumed to be normally distributed. Given 95% likelihood, the exit velocity is calculated to be in the range between 1526 m/sec and 1575 m/sec, the axial acceleration between 80,170 g and 90,735 g, and the maximum von Mises stress between 894 MPa and 1009 MPa. Although the deviation of the exit velocity was not substantial, the flight range and performance could be of concern for a high precision ammunition system such as EAPS. The stress responses differed by more than 100 MPa. Care must be taken to avoid local failure because of the pressure deviations. Finally, the variations of the responses may serve as a guideline for the design of the EAPS projectile system. In addition, the ranges of the responses should be anticipated from experimental results even in a regular shooting environment.

6. References

1. Chen, M. *Structural Design and Analysis of Initial Extended Area Protection and Survivability (EAPS) Projectile Configurations*; ARL-TR-3866; U.S. Army Research Laboratory: Aberdeen Proving Ground, MD, August 2006.

2. Chen, M. Structural Design and Analysis of Hit-to-Kill Projectile. 9th International LS-DYNA Users Conference, Dearborn, Michigan, USA, Session 2, 13-22, 2006.

3. Chen, M. *Design of Experiments Study of Initial Extended Area Protection and Survivability (EAPS) Projectile System*; ARL-TR-4109; U.S. Army Research Laboratory: Aberdeen Proving Ground, MD, 2007.

4. Anderson, R.; Fickie, K. *IBHVG2 (Interior Ballistics of High Velocity Guns, Version 2) – A User's Guide*; BRL-TR-2829; U.S. Army Ballistics Research Laboratory: Aberdeen Proving Ground, MD, July 1987.

5. Gough, P. S. *The XNOVAKTC Code*; BRL-CR-627, U.S. Army Ballistics Research Laboratory: Aberdeen Proving Ground, MD, February 1990.

6. Ruth, C.; Minor, T. *Experimental Study of Flame Spreading Processes in 155-mm, XM 216 Modular Propelling Charges*; BRL-MR-3840; U.S. Army Ballistics Research Laboratory: Aberdeen Proving Ground, MD, June 1990.

7. Gough, P. S. *Initial Development of the Core Module of Next Generation Model NGEN*; ARL-CR-234; U.S. Army Ballistics Research Laboratory: Aberdeen Proving Ground, MD, June 1995.

8. Nusca, M. *High-Performance Computing and Simulation for Advanced Armament Propulsion*; ARL-TR-3215; U.S. Army Research Laboratory: Aberdeen Proving Ground, MD, June 2004.

9. Nusca M.; Horst, A.; Newill, J. *Multidimensional, Two Phase Simulations Of National Telescoped Ammunition Propelling Charge*; ARL-TR-3306; U.S. Army Research Laboratory: Aberdeen Proving Ground, MD, September 2004.

10. Chang, L.-M. Personal communication, Propulsion Science Branch, U.S. Army Research Laboratory: Aberdeen Proving Ground, MD, 2 August 2006.

INTENTIONALLY LEFT BLANK

Appendix A. Monte Carlo Simulated Pressure-Time (MPa) History at the Base of EAPS Projectile

Time Step	Simulation Run Number																
	1	2	3	4	5	6	7	8	9	10	11	12	13	14	15	16	17
0.1	0.44	0.43	0.43	0.44	0.45	0.44	0.41	0.42	0.45	0.45	0.42	0.44	0.45	0.43	0.43	0.44	0.43
0.2	1.18	1.19	1.18	1.21	1.28	1.16	1.24	1.18	1.16	1.16	1.19	1.23	1.16	1.17	1.22	1.20	1.19
0.3	2.52	2.51	2.57	2.50	2.59	2.47	2.51	2.48	2.53	2.45	2.34	2.48	2.58	2.45	2.53	2.54	2.56
0.4	4.56	4.68	4.54	4.57	4.83	4.52	4.82	4.43	4.45	4.70	4.55	4.56	4.64	4.56	4.40	4.53	4.42
0.5	7.73	7.73	7.81	8.08	8.09	8.07	7.75	8.02	7.97	7.64	7.78	8.45	7.89	7.76	8.43	8.13	8.03
0.6	13.48	13.70	13.62	13.20	13.84	13.61	12.30	13.32	13.45	13.76	13.41	13.41	13.36	13.01	12.58	13.15	12.98
0.7	20.54	21.96	21.74	21.16	21.97	21.92	21.84	21.25	20.04	21.43	21.23	20.52	21.22	21.83	21.16	22.42	21.55
0.8	32.07	30.27	31.12	33.66	32.07	30.58	32.19	30.48	33.82	31.78	33.20	34.08	31.68	31.11	31.18	31.81	32.31
0.9	44.96	45.40	47.82	47.00	44.86	46.08	45.76	44.82	46.57	46.49	44.35	44.60	43.70	45.82	44.13	49.44	47.78
1	61.52	62.19	61.75	62.34	62.35	66.67	62.03	64.86	62.33	64.11	60.68	62.05	64.06	61.37	61.70	63.14	61.08
1.1	78.23	90.14	85.48	87.93	81.90	84.27	83.29	85.23	87.61	88.39	84.30	85.27	84.75	88.35	80.28	84.48	84.87
1.2	113.0	111.6	113.5	113.5	115.8	113.1	115.9	108.5	114.0	118.3	119.1	107.3	115.4	110.9	111.0	113.6	110.2
1.3	145.3	155.8	135.3	140.9	146.3	141.2	150.3	149.9	148.1	144.9	149.1	150.1	144.5	141.2	150.1	144.8	147.7
1.4	190.8	179.8	179.2	187.1	172.2	179.8	184.4	170.6	171.4	173.2	177.4	179.6	179.6	178.2	179.8	183.6	179.5
1.5	214.1	224.1	227.5	212.9	225.2	230.3	220.0	208.9	222.1	206.0	214.0	223.3	208.7	220.3	212.7	208.5	208.6
1.6	260.0	256.1	251.3	247.5	256.9	253.5	260.4	259.8	261.7	265.4	249.4	253.4	264.4	256.8	260.1	247.8	262.9
1.7	270.1	276.5	279.1	278.5	285.7	295.1	264.8	286.1	275.9	279.3	273.7	291.9	281.8	269.9	282.8	289.2	273.4
1.8	287.9	288.3	297.5	302.2	301.1	296.5	291.1	297.1	312.9	298.7	290.1	301.1	305.4	298.9	290.0	308.2	299.3
1.9	316.2	314.2	298.8	313.4	313.0	320.7	315.2	301.7	316.0	306.5	319.5	302.3	321.5	307.8	307.5	305.9	313.3
2	302.9	330.3	292.1	315.8	321.6	330.2	312.1	323.2	308.2	309.3	309.3	316.1	314.1	315.1	314.2	329.7	318.9
2.1	305.0	311.6	308.7	306.0	308.4	315.2	310.8	300.4	308.4	318.4	307.1	324.2	296.7	308.2	324.2	317.4	319.1
2.2	315.7	282.7	306.8	298.6	298.4	310.9	301.7	307.3	289.6	295.8	294.2	307.9	295.0	302.9	297.3	306.7	300.7
2.3	285.5	291.2	290.4	300.4	288.6	293.6	285.0	296.3	285.0	291.0	296.4	285.9	283.6	305.4	301.8	282.6	285.7
2.4	274.0	275.0	283.4	278.8	267.1	280.5	281.9	265.4	273.7	276.0	276.3	269.6	279.2	262.6	278.2	288.2	275.2
2.5	265.9	263.0	270.5	249.3	252.8	251.9	247.8	243.2	255.4	254.4	251.3	263.1	266.1	250.7	264.1	257.9	241.7
2.6	229.9	233.8	226.0	229.6	232.6	231.1	236.8	223.3	227.1	228.8	235.5	242.2	226.8	228.6	238.1	223.3	238.2
2.7	199.4	204.5	198.1	202.8	197.8	201.6	213.0	202.7	203.8	194.8	219.4	208.4	206.7	219.6	198.8	212.7	214.2
2.8	178.1	183.8	184.3	183.6	187.1	189.9	187.0	179.9	188.9	191.0	189.8	183.7	183.1	179.2	192.6	181.1	172.8
2.9	165.6	174.0	164.0	157.3	156.3	166.2	170.5	159.0	170.4	167.1	168.9	165.3	159.6	164.3	165.8	167.2	156.0
3	150.8	147.7	147.8	154.8	150.3	146.6	147.5	146.9	153.6	150.5	154.6	145.0	137.6	144.7	146.9	147.5	149.3
3.1	132.2	128.3	138.8	127.5	139.0	134.6	134.0	135.7	129.8	134.5	139.5	130.9	134.3	134.5	125.0	126.0	135.4
3.2	113.8	116.1	121.1	117.7	127.7	121.2	122.4	123.4	122.3	122.0	125.2	115.6	121.6	119.4	128.4	122.3	127.0
3.3	109.6	106.3	104.1	108.0	112.1	104.4	104.5	105.9	111.8	113.8	108.5	109.6	106.8	101.6	110.5	108.1	111.5
3.4	102.5	98.0	101.1	103.6	100.7	105.4	100.3	100.9	100.8	101.2	102.3	97.6	96.8	93.6	98.1	95.6	97.9
3.5	88.21	91.32	92.18	97.87	93.37	91.01	93.48	87.51	85.04	86.96	90.35	95.71	85.91	99.66	83.63	89.32	88.77
3.6	82.22	81.99	84.24	83.24	85.40	82.50	84.29	85.88	83.23	79.63	87.13	83.82	83.26	85.16	83.06	82.55	80.21
3.7	77.62	78.33	77.47	77.77	73.50	74.59	82.72	82.54	77.56	77.48	74.04	77.06	79.23	77.07	74.39	79.76	72.37
3.8	72.86	71.61	71.78	72.32	67.47	70.80	70.67	71.57	68.19	72.06	75.67	68.99	75.57	68.95	72.30	72.78	73.35
3.9	70.68	66.25	66.71	65.79	64.93	63.15	67.52	63.36	64.85	64.89	63.63	67.13	65.24	68.37	69.58	65.35	65.19
4	59.78	59.07	60.86	66.86	61.76	64.40	64.87	61.37	62.95	60.84	61.12	62.44	63.14	63.09	63.98	59.03	61.46
4.1	56.40	56.41	58.06	58.34	58.38	55.71	57.52	56.62	59.51	57.62	59.36	60.38	58.28	58.67	57.59	58.50	57.05
4.2	55.21	55.53	55.73	56.40	51.99	57.32	50.73	49.10	52.07	54.18	56.12	54.11	57.77	56.05	54.67	53.88	56.29
4.3	53.18	49.42	52.11	49.84	52.36	52.54	50.25	49.45	52.36	50.12	49.68	49.62	49.67	54.30	51.24	50.04	50.55
4.4	46.52	49.17	50.14	49.32	48.82	48.21	44.51	50.03	48.80	48.89	48.90	48.64	46.58	47.66	49.07	48.20	47.13
4.5	45.38	43.84	42.35	45.55	43.78	46.27	46.08	45.25	44.74	44.27	45.18	43.30	45.02	45.36	43.33	45.06	42.62
4.6	42.03	42.02	42.89	41.52	44.13	45.07	43.82	42.35	41.29	43.65	43.52	44.21	45.00	43.90	42.66	44.47	43.13
4.7	38.84	40.07	38.53	41.46	41.62	40.88	37.75	39.29	40.38	41.13	37.88	38.50	39.40	41.22	40.24	41.23	42.27

Time Step	Simulation Run Number																
	18	19	20	21	22	23	24	25	26	27	28	29	30	31	32	33	34
0.1	0.43	0.43	0.42	0.43	0.45	0.43	0.42	0.43	0.40	0.42	0.45	0.43	0.42	0.44	0.45	0.44	0.43
0.2	1.23	1.22	1.30	1.17	1.21	1.23	1.20	1.13	1.25	1.20	1.24	1.21	1.17	1.12	1.17	1.16	1.16
0.3	2.46	2.64	2.55	2.42	2.56	2.58	2.52	2.44	2.54	2.53	2.52	2.51	2.52	2.55	2.53	2.49	2.48
0.4	4.63	4.47	4.42	4.53	4.47	4.59	4.57	4.62	4.53	4.29	4.62	4.52	4.32	4.61	4.54	4.58	4.49
0.5	8.12	7.83	8.11	7.98	7.91	7.96	7.71	8.17	7.70	7.93	7.70	8.31	7.85	8.11	7.83	7.94	8.23
0.6	13.31	13.48	13.22	13.01	13.29	13.10	12.83	13.39	13.92	12.78	13.93	13.82	13.28	12.87	13.89	13.32	13.10
0.7	21.29	21.25	21.11	21.66	22.72	21.44	20.87	22.90	22.16	21.21	21.59	20.83	21.33	21.72	21.69	21.68	22.56
0.8	31.70	30.43	31.16	31.60	32.51	34.92	32.88	31.48	33.62	30.99	30.97	32.33	31.49	31.36	32.08	31.96	31.76
0.9	47.55	45.00	46.33	44.52	45.27	44.35	48.83	45.36	43.76	46.14	46.04	48.83	47.12	45.19	45.97	45.39	45.90
1	60.44	65.78	65.35	63.06	62.75	66.05	65.53	61.41	63.23	65.34	65.57	64.85	57.64	66.84	62.70	64.94	63.17
1.1	82.28	87.83	83.87	84.60	87.28	83.49	88.28	84.92	88.24	82.14	87.56	88.35	83.02	86.10	86.88	84.02	90.18
1.2	119.1	110.4	119.1	116.6	111.2	114.7	108.2	113.1	115.7	114.2	112.5	116.2	112.9	116.9	107.8	116.0	111.3
1.3	150.1	153.9	141.6	147.9	143.4	143.1	143.0	145.3	144.3	143.1	148.2	140.4	147.2	147.4	140.6	147.3	145.9
1.4	185.9	190.5	180.3	175.4	183.4	181.0	176.1	184.7	181.7	172.3	184.9	182.7	177.1	191.5	175.8	186.4	186.0
1.5	222.1	212.0	211.2	225.6	213.1	222.0	211.4	203.9	217.8	224.4	217.0	228.2	218.4	223.1	218.6	220.2	208.3
1.6	245.4	234.2	256.5	250.8	243.6	250.5	242.8	257.8	264.2	256.4	255.5	256.7	250.0	250.5	248.4	257.5	257.4
1.7	292.0	279.3	271.0	288.3	286.1	281.5	282.7	278.0	278.9	275.1	272.0	278.6	294.0	273.3	283.2	281.2	277.7
1.8	315.5	313.6	310.7	302.5	295.0	312.7	302.6	324.6	305.7	302.0	300.4	293.9	301.2	303.4	292.8	281.9	296.3
1.9	316.7	299.4	326.9	312.2	293.0	305.7	312.7	313.4	308.5	311.2	306.9	303.0	303.1	308.8	307.7	314.1	315.6
2	301.1	318.7	320.3	311.7	323.8	320.3	310.2	313.6	327.4	311.3	320.8	310.2	322.1	310.1	305.2	322.2	318.2
2.1	305.2	309.6	320.4	317.5	300.3	301.8	308.1	296.4	310.9	307.8	319.1	319.0	304.6	315.7	304.6	312.8	301.5
2.2	304.1	305.3	301.2	309.2	314.4	288.3	298.4	320.7	321.2	299.9	295.8	303.7	289.1	309.9	298.5	303.3	290.0
2.3	289.4	292.6	298.1	301.2	299.1	291.9	291.9	279.8	299.2	300.9	274.9	290.4	287.9	296.1	303.1	289.9	296.1
2.4	277.1	257.1	270.6	269.1	286.6	272.4	280.0	282.3	282.2	277.9	282.0	274.4	280.2	275.9	281.0	291.2	282.9
2.5	248.5	259.1	254.3	259.4	267.7	255.1	259.3	252.9	261.6	258.2	255.2	260.1	258.4	263.3	247.5	250.5	257.2
2.6	227.8	225.1	237.3	241.3	245.7	237.7	234.7	224.5	232.8	222.9	219.4	227.1	209.0	231.3	225.3	245.1	235.6
2.7	203.6	209.9	200.2	217.0	203.6	205.3	196.5	201.5	202.5	203.4	218.7	207.4	206.2	198.2	203.8	205.3	198.3
2.8	186.1	183.4	177.8	183.4	193.6	182.7	179.7	182.5	182.6	186.6	189.4	178.1	191.2	199.7	180.1	178.9	183.1
2.9	159.5	163.2	171.2	161.8	165.9	163.2	157.3	164.5	163.2	170.2	167.0	175.4	165.2	161.8	173.6	161.7	167.0
3	146.2	146.8	155.2	147.8	151.7	151.1	145.0	150.4	147.2	155.5	144.2	156.7	144.9	151.0	153.0	144.6	150.1
3.1	134.2	139.7	128.6	132.0	137.6	130.1	136.0	127.1	133.4	132.7	126.8	133.7	135.8	128.7	132.8	134.2	134.4
3.2	116.0	118.3	115.5	123.5	119.0	119.1	117.2	123.5	120.1	118.9	120.4	123.3	117.8	129.4	127.3	116.6	121.8
3.3	109.0	112.6	114.0	109.8	111.7	102.8	106.5	114.4	107.0	108.7	110.1	108.7	108.7	111.8	112.6	113.2	111.0
3.4	98.5	102.0	100.1	97.0	100.8	98.6	95.3	98.9	96.9	96.5	101.0	96.6	103.5	97.9	96.3	98.7	96.8
3.5	83.24	86.75	91.26	85.79	89.18	87.37	89.56	93.34	88.34	95.49	95.40	87.54	96.91	97.59	86.77	87.56	92.39
3.6	85.13	84.40	84.21	79.23	87.31	79.13	83.69	80.66	81.47	85.79	84.11	83.99	82.16	84.16	80.94	82.24	86.39
3.7	78.78	76.07	84.64	78.74	72.45	76.05	76.97	76.91	77.60	74.29	74.52	75.21	72.60	77.70	80.49	74.18	72.83
3.8	72.81	73.10	71.44	71.92	73.03	72.17	71.64	68.78	72.65	71.57	76.08	70.03	70.20	76.00	73.01	71.02	69.05
3.9	68.16	67.68	64.20	68.66	66.37	64.64	65.76	69.47	67.32	65.60	66.55	67.34	64.05	65.67	65.00	62.73	68.15
4	63.51	62.86	58.68	60.45	60.51	60.74	61.78	61.47	64.34	63.09	60.68	62.57	62.17	61.99	65.89	60.72	61.64
4.1	59.70	60.99	57.03	56.79	56.58	54.63	58.12	53.39	62.12	57.24	59.45	55.89	57.38	59.73	57.51	59.23	61.73
4.2	54.07	56.15	55.38	57.43	55.07	53.79	54.70	53.33	49.81	51.96	50.10	53.42	53.37	55.46	54.32	52.80	52.89
4.3	50.00	51.47	50.73	52.24	53.30	51.99	51.45	53.28	51.30	52.30	51.73	50.08	51.58	51.09	47.44	50.32	49.67
4.4	48.13	46.16	48.14	48.94	45.77	45.87	47.44	46.29	47.52	49.02	48.16	45.08	45.38	47.45	44.77	46.96	48.96
4.5	46.66	44.01	46.71	44.16	45.92	43.32	45.26	44.86	43.76	44.74	43.03	44.15	45.80	43.64	46.42	43.92	45.27
4.6	41.51	41.57	44.34	42.82	42.23	42.96	40.93	42.21	41.32	40.26	43.06	44.07	43.58	43.73	42.27	41.87	43.43
4.7	39.81	39.77	40.23	39.99	40.57	39.60	42.13	38.38	39.30	40.97	39.06	40.71	39.33	39.40	40.43	41.46	40.81

Time Step	Simulation Run Number															
	35	36	37	38	39	40	41	42	43	44	45	46	47	48	49	50
0.1	0.45	0.44	0.43	0.43	0.41	0.43	0.45	0.42	0.43	0.42	0.45	0.46	0.43	0.44	0.44	0.42
0.2	1.22	1.22	1.11	1.15	1.20	1.18	1.21	1.20	1.16	1.19	1.23	1.17	1.17	1.16	1.13	1.16
0.3	2.49	2.62	2.49	2.52	2.57	2.60	2.46	2.52	2.56	2.42	2.49	2.56	2.61	2.56	2.46	2.39
0.4	4.52	4.48	4.58	4.29	4.62	4.53	4.43	4.69	4.74	4.67	4.54	4.58	4.43	4.32	4.58	4.48
0.5	7.69	8.28	7.43	7.83	7.53	7.85	7.88	7.91	8.36	8.15	8.12	8.05	7.81	8.13	7.91	7.79
0.6	13.17	13.63	13.59	13.53	13.28	13.81	13.42	13.08	13.35	14.32	12.95	12.88	13.51	13.03	12.90	13.24
0.7	20.90	21.49	21.51	21.71	21.48	20.69	20.00	21.27	21.01	21.88	22.30	20.40	22.37	20.16	22.36	21.37
0.8	32.08	30.68	32.04	32.05	32.68	33.60	31.47	33.03	32.26	33.08	32.24	31.58	33.06	32.34	33.00	33.27
0.9	45.90	44.90	44.12	45.53	43.65	45.83	45.41	47.87	44.59	45.91	45.35	43.76	46.53	45.96	44.63	46.46
1	62.57	59.12	61.86	63.29	62.96	61.48	64.58	64.01	64.20	65.21	62.63	63.14	62.95	62.93	63.43	63.05
1.1	86.42	87.18	85.67	86.74	86.26	81.97	85.52	84.89	85.46	81.01	82.25	87.25	83.51	86.04	81.64	86.70
1.2	106.7	113.3	111.8	108.1	110.1	111.2	109.8	109.4	118.9	108.9	112.4	117.3	111.7	115.1	105.1	111.4
1.3	139.7	138.3	136.8	143.7	139.0	145.4	146.3	144.6	141.9	144.4	145.1	149.2	146.7	145.2	138.9	148.2
1.4	192.2	191.4	184.1	181.0	178.7	180.3	190.0	189.1	180.5	180.0	177.1	179.5	180.1	175.9	184.2	190.2
1.5	217.6	226.6	212.3	227.8	218.9	219.4	212.2	222.4	217.0	218.5	223.3	208.3	218.4	215.7	212.4	222.5
1.6	261.0	252.6	245.2	255.8	242.8	258.1	253.6	250.9	248.2	250.0	242.3	243.8	263.9	262.8	255.6	242.4
1.7	298.4	273.9	287.7	276.4	277.9	305.2	280.4	269.7	279.3	270.9	272.0	284.1	278.3	273.1	276.5	278.7
1.8	303.1	303.8	318.9	303.6	292.9	285.5	300.0	308.9	288.9	297.9	279.4	311.6	303.2	300.4	305.8	290.9
1.9	327.4	319.8	318.9	327.8	310.8	317.9	310.6	299.7	312.9	318.2	302.6	318.7	322.6	295.1	298.4	307.5
2	316.9	312.2	330.5	337.1	334.3	330.6	297.8	331.4	303.4	312.6	325.4	329.1	316.9	333.9	299.5	315.0
2.1	318.4	315.8	317.5	321.4	298.3	314.5	316.5	305.2	304.0	316.1	299.4	313.4	319.9	294.8	323.0	312.8
2.2	315.6	297.5	298.9	294.9	303.1	299.5	282.3	300.9	295.8	302.0	314.9	320.1	324.4	303.2	292.7	318.9
2.3	269.4	294.7	285.5	293.2	289.3	290.7	294.4	271.4	292.7	297.6	269.6	305.9	298.1	289.0	287.4	288.7
2.4	279.1	287.0	283.4	291.4	277.4	283.2	277.2	275.4	299.0	284.9	278.6	274.9	291.2	284.0	261.0	267.0
2.5	252.9	258.9	260.3	264.5	252.8	248.7	258.9	247.6	261.1	240.0	273.0	252.0	255.7	240.8	258.6	250.0
2.6	240.5	232.2	228.0	229.8	240.1	220.7	237.3	227.8	228.0	226.7	223.3	221.8	235.0	242.9	234.9	222.5
2.7	213.4	215.0	210.5	215.4	193.0	206.6	208.1	199.6	204.7	204.5	210.0	207.0	206.9	215.8	209.5	205.8
2.8	190.1	179.3	193.9	179.8	182.9	191.3	187.4	188.5	185.9	180.2	186.2	182.1	187.7	191.3	180.3	190.3
2.9	160.1	162.3	164.7	162.8	160.5	162.1	161.6	167.3	161.0	164.5	173.9	166.6	172.9	168.6	165.4	163.7
3	154.6	142.3	154.7	148.7	144.3	152.0	142.2	147.7	150.5	141.2	150.0	154.6	147.6	150.7	144.9	152.4
3.1	124.8	138.9	135.4	139.5	126.8	128.5	128.9	136.2	133.2	131.6	130.5	134.8	135.7	132.1	129.9	133.8
3.2	122.9	122.2	111.7	119.6	123.9	120.0	121.2	125.9	119.7	117.6	110.5	118.0	124.2	118.9	119.6	116.6
3.3	103.8	112.9	107.2	107.1	115.6	112.0	104.8	102.4	104.2	105.0	110.8	100.9	107.2	105.8	108.2	112.1
3.4	99.6	98.1	100.9	100.9	101.1	100.0	101.9	103.0	97.4	102.9	98.4	105.9	98.8	103.8	104.6	100.8
3.5	87.61	94.00	89.25	88.24	97.01	89.39	92.97	87.53	89.56	89.28	88.22	93.44	91.27	85.43	88.02	93.72
3.6	86.61	78.43	80.13	82.20	81.32	86.52	83.33	80.35	83.00	85.39	77.77	81.08	87.13	81.74	83.71	84.47
3.7	76.81	76.28	75.71	79.39	80.57	76.07	76.80	75.02	76.22	74.48	75.44	71.75	74.31	78.61	74.40	81.85
3.8	68.22	68.65	68.69	73.84	70.60	73.09	67.71	70.72	71.36	70.62	70.49	70.47	70.61	72.46	71.78	71.08
3.9	62.99	64.47	66.93	70.77	65.20	70.61	69.28	69.47	71.67	67.06	63.16	66.81	69.08	65.75	64.01	66.11
4	60.71	59.15	62.93	64.76	61.85	62.34	61.74	57.86	61.08	59.91	63.28	61.13	60.16	61.11	63.54	60.12
4.1	57.45	58.88	57.61	58.78	57.51	59.13	57.72	60.32	57.32	62.32	60.39	56.30	56.05	58.93	57.16	56.35
4.2	53.89	54.92	53.18	53.54	53.47	54.41	52.84	54.28	51.29	55.39	54.23	53.40	53.94	54.81	51.93	57.16
4.3	51.02	49.49	50.33	51.55	51.16	49.82	49.53	51.18	49.70	51.76	47.49	49.20	48.45	52.01	49.76	48.32
4.4	46.15	48.55	46.53	49.11	49.02	48.66	49.06	48.49	46.75	46.54	49.14	48.49	47.35	47.23	48.16	47.30
4.5	43.20	47.57	43.95	44.84	44.54	46.89	44.16	47.06	44.19	44.33	45.18	44.57	42.98	44.92	45.76	43.40
4.6	42.14	41.42	42.08	45.16	45.22	43.70	43.10	45.51	43.45	41.85	41.18	44.07	42.82	43.37	42.68	42.10
4.7	40.19	39.86	39.49	41.12	40.32	40.44	39.47	41.95	42.53	40.29	40.59	41.54	40.18	39.49	40.79	42.20

Time Step	Simulation Run Number																
	51	52	53	54	55	56	57	58	59	60	61	62	63	64	65	66	67
0.1	0.44	0.46	0.43	0.42	0.42	0.42	0.48	0.42	0.46	0.43	0.45	0.44	0.45	0.44	0.43	0.43	0.43
0.2	1.23	1.22	1.18	1.13	1.24	1.17	1.16	1.20	1.17	1.14	1.23	1.22	1.24	1.23	1.21	1.19	1.19
0.3	2.48	2.51	2.50	2.56	2.53	2.53	2.53	2.40	2.39	2.49	2.36	2.36	2.50	2.48	2.57	2.39	2.59
0.4	4.69	4.62	4.45	4.55	4.60	4.64	4.35	4.60	4.53	4.49	4.56	4.44	4.41	4.67	4.65	4.78	4.57
0.5	7.57	8.14	7.64	7.98	7.90	7.92	8.07	7.90	8.13	7.84	8.46	7.84	7.67	7.87	8.04	8.02	7.86
0.6	13.52	12.80	13.12	13.38	13.77	12.92	13.98	13.42	13.19	13.67	13.11	12.90	13.18	13.15	13.59	13.42	13.52
0.7	21.15	21.08	21.84	21.92	22.02	20.94	22.10	21.29	21.39	22.48	22.20	22.80	22.43	21.85	22.53	20.37	21.10
0.8	32.10	32.44	30.36	31.66	32.25	32.42	32.21	30.27	32.84	32.35	31.97	32.95	31.60	31.85	31.96	32.76	31.91
0.9	46.64	43.54	45.03	44.44	47.30	45.14	45.41	48.16	47.23	46.27	44.97	43.35	46.17	43.86	45.14	45.24	44.15
1	63.57	63.18	64.95	62.97	62.65	62.93	62.64	63.62	62.93	61.78	62.64	64.47	62.46	63.70	63.62	65.71	63.12
1.1	84.96	85.10	84.27	86.30	86.51	84.59	81.51	84.31	85.99	85.46	89.21	85.80	78.12	84.72	82.62	86.41	83.91
1.2	113.7	104.2	111.1	111.4	109.6	111.6	115.3	111.4	113.2	115.0	112.1	115.4	114.9	115.1	109.1	109.7	114.9
1.3	139.4	141.8	141.3	153.1	152.3	145.6	149.0	151.2	144.2	150.9	148.5	144.1	148.1	139.9	146.7	145.9	138.7
1.4	182.8	182.8	184.3	184.9	184.9	191.1	185.4	182.0	176.8	169.7	176.6	193.9	182.0	176.3	170.1	178.0	180.8
1.5	208.4	217.4	218.5	223.7	213.5	213.0	211.1	216.5	220.4	226.4	219.7	224.5	213.9	223.2	215.9	221.2	216.4
1.6	263.3	244.9	263.0	240.2	259.7	262.5	240.7	263.5	244.2	268.0	251.3	263.9	250.8	250.3	253.3	259.6	260.1
1.7	284.7	287.5	273.8	277.6	285.3	292.1	290.6	290.5	270.9	284.0	264.6	286.3	281.2	278.6	278.9	284.9	275.0
1.8	292.1	305.2	296.6	304.2	307.9	298.8	301.1	301.5	298.8	313.3	303.7	315.2	300.5	298.9	305.8	309.8	298.1
1.9	296.4	323.3	321.4	320.8	308.7	310.4	314.1	315.9	327.6	315.8	313.0	310.0	288.0	304.7	310.1	310.0	312.5
2	324.4	315.6	302.3	312.1	302.3	318.6	323.1	334.2	305.3	321.0	331.3	309.1	296.2	327.4	298.7	321.7	317.3
2.1	305.7	310.7	296.4	302.9	314.2	307.7	303.3	294.5	308.1	319.3	307.9	308.8	319.1	324.2	311.6	309.3	320.4
2.2	298.5	298.6	317.5	293.6	312.2	290.6	299.7	299.8	308.7	299.2	303.5	295.1	297.4	291.6	295.3	311.1	325.4
2.3	310.8	299.7	280.2	291.6	307.4	277.0	295.3	288.2	288.5	296.6	284.4	275.9	281.0	294.0	273.0	281.3	281.0
2.4	274.1	277.3	257.3	283.7	290.0	289.9	262.4	262.6	266.4	272.9	287.5	279.9	296.5	282.4	275.1	281.3	263.9
2.5	254.9	248.3	257.5	247.7	246.3	254.7	256.7	259.6	253.5	253.8	271.1	251.3	258.3	252.1	247.6	257.3	247.0
2.6	223.5	219.6	228.8	221.5	234.8	233.2	239.9	236.8	234.2	239.6	225.7	232.5	239.0	225.5	236.8	241.2	229.0
2.7	215.0	206.1	210.5	211.4	213.7	215.3	202.9	211.1	204.4	196.7	206.5	199.0	213.9	209.3	210.6	204.9	215.8
2.8	178.5	187.1	196.1	182.0	188.0	188.0	172.6	186.3	181.7	189.9	184.2	174.5	182.9	183.6	185.4	186.3	181.4
2.9	165.3	166.3	164.4	166.1	167.2	164.4	176.1	164.5	163.1	161.6	151.8	168.1	160.5	164.4	166.5	170.9	166.6
3	141.8	156.0	150.3	151.2	153.3	148.0	137.4	154.2	147.3	146.3	149.9	150.9	150.2	143.4	153.0	148.3	145.4
3.1	129.1	135.3	133.7	131.1	133.3	141.1	132.6	126.3	139.5	128.2	129.2	132.8	137.6	128.8	133.9	135.9	137.1
3.2	122.0	120.0	117.5	120.0	116.2	116.8	121.2	125.5	121.6	111.8	122.5	121.3	120.0	112.8	115.3	118.7	120.5
3.3	110.2	110.4	104.2	113.8	110.0	108.0	101.8	111.6	106.0	106.3	105.4	106.7	110.1	113.2	109.2	115.2	112.1
3.4	100.9	93.5	95.9	103.0	100.2	93.3	97.5	98.8	97.0	99.9	103.6	102.6	101.7	100.5	102.9	94.1	98.3
3.5	89.41	92.69	89.01	82.88	93.42	93.03	93.22	92.76	92.71	93.04	87.72	92.78	93.44	88.63	93.09	93.85	90.64
3.6	88.42	83.77	83.04	86.76	82.16	86.16	84.76	82.60	83.98	86.46	89.43	81.86	81.32	87.08	85.47	82.72	86.70
3.7	76.43	76.15	74.60	78.30	77.82	78.45	79.07	73.83	77.60	78.85	79.84	73.19	78.89	77.02	78.34	77.20	76.86
3.8	68.46	73.96	70.18	68.10	72.37	71.44	71.10	70.17	71.61	72.58	70.69	74.42	69.31	69.64	73.97	70.71	72.35
3.9	69.45	65.91	68.13	66.52	63.91	64.65	65.38	67.11	65.89	66.83	65.04	68.12	63.95	67.92	70.81	67.59	64.96
4	60.42	59.32	62.13	61.03	63.70	60.11	61.65	64.64	62.12	59.19	61.10	62.43	62.08	63.94	63.12	61.57	63.53
4.1	56.22	56.33	58.13	54.15	57.46	56.17	58.04	59.78	56.55	59.51	58.09	58.41	56.27	56.33	54.44	55.80	59.76
4.2	56.18	53.41	55.07	53.63	55.47	54.18	54.72	55.97	51.53	53.12	54.57	56.88	53.49	56.45	55.40	55.25	54.44
4.3	50.45	50.91	50.16	51.35	50.51	51.05	52.70	51.72	51.55	49.25	50.87	49.05	50.72	52.10	51.92	50.62	50.69
4.4	47.00	46.07	48.81	50.47	49.01	49.94	47.80	46.01	48.12	45.49	46.26	49.31	48.28	45.78	47.25	50.45	49.47
4.5	44.63	44.74	44.93	42.22	44.06	45.72	46.54	46.52	43.16	45.00	45.80	46.67	43.88	45.42	42.95	46.60	45.20
4.6	42.00	42.62	42.17	42.75	45.08	41.01	42.37	41.46	44.09	41.63	42.05	43.20	43.18	43.87	42.89	43.32	41.87
4.7	39.89	38.73	41.50	41.06	38.84	41.17	40.02	41.35	38.98	42.64	40.33	41.40	40.82	40.96	41.84	38.40	42.50

Time Step	Simulation Run Number																
	68	69	70	71	72	73	74	75	76	77	78	79	80	81	82	83	84
0.1	0.43	0.41	0.43	0.44	0.41	0.42	0.43	0.42	0.42	0.43	0.42	0.45	0.41	0.44	0.43	0.43	0.44
0.2	1.18	1.23	1.10	1.23	1.16	1.20	1.23	1.17	1.17	1.24	1.26	1.18	1.19	1.14	1.23	1.12	1.21
0.3	2.63	2.48	2.47	2.43	2.51	2.52	2.54	2.57	2.57	2.38	2.46	2.47	2.47	2.50	2.48	2.58	2.48
0.4	4.53	4.62	4.66	4.70	4.50	4.62	4.48	4.53	4.65	4.32	4.62	4.56	4.36	4.47	4.54	4.64	4.35
0.5	7.89	7.84	8.12	8.25	8.05	8.11	7.71	8.03	8.11	8.21	8.05	7.88	7.33	8.02	7.54	7.72	7.79
0.6	13.35	13.13	13.71	14.28	13.36	13.85	12.83	13.84	13.21	13.47	13.97	12.97	13.75	13.86	13.32	13.16	12.85
0.7	21.81	21.72	20.61	21.38	20.79	21.81	21.85	22.01	20.75	21.07	21.67	21.46	20.86	21.09	21.72	21.58	21.07
0.8	32.19	32.79	32.43	31.87	31.01	31.84	34.15	33.57	30.02	32.15	32.18	33.45	32.47	33.21	29.71	32.55	31.97
0.9	45.62	45.95	45.16	46.76	42.91	45.34	43.03	44.95	45.44	44.80	45.06	44.12	44.86	47.84	44.60	45.42	47.47
1	64.92	65.21	63.39	62.51	63.34	63.24	63.13	65.50	60.80	63.91	62.14	66.60	63.20	67.10	64.29	61.89	61.92
1.1	86.98	84.06	82.76	86.38	84.72	84.67	87.98	88.63	90.03	89.21	85.01	87.92	84.36	87.43	87.71	85.81	88.29
1.2	112.1	110.8	111.8	112.0	113.2	112.3	112.8	113.3	113.5	111.2	111.5	114.1	119.5	119.0	116.0	113.9	117.1
1.3	151.0	147.4	141.9	146.0	147.5	142.4	154.7	143.2	139.9	141.1	147.8	155.8	145.8	151.1	144.9	151.0	143.7
1.4	176.8	187.8	196.4	188.4	170.4	172.0	184.1	177.9	177.7	174.7	177.1	178.0	180.2	184.6	179.9	181.6	183.9
1.5	200.8	224.5	223.0	207.8	213.5	229.3	222.4	214.0	229.2	213.4	216.4	212.2	224.7	221.4	217.3	218.1	222.1
1.6	250.6	262.8	258.1	250.5	239.1	247.5	255.7	244.8	262.8	259.6	251.9	259.2	253.7	248.3	241.4	255.5	249.0
1.7	284.0	285.8	279.8	260.7	281.7	276.2	275.7	276.2	288.4	271.2	289.5	286.2	283.2	284.7	281.9	274.5	289.3
1.8	293.3	284.6	302.3	300.4	285.1	305.6	313.5	305.8	319.9	301.8	297.1	295.7	312.2	298.3	295.7	297.4	293.7
1.9	315.5	333.2	301.3	310.6	308.1	300.4	303.6	322.7	309.6	314.9	318.4	310.8	304.4	303.6	307.2	312.6	312.9
2	300.4	305.7	318.2	313.9	309.1	321.8	309.2	316.7	299.3	299.2	313.4	327.7	309.3	305.6	325.0	311.0	321.6
2.1	321.2	313.0	298.5	303.6	314.5	307.8	304.7	316.9	299.7	319.2	298.4	312.2	305.3	300.5	326.2	309.2	306.5
2.2	305.8	303.8	307.3	306.5	307.5	299.4	307.3	299.5	319.8	309.4	310.3	311.3	299.9	303.9	308.8	286.7	305.9
2.3	277.8	304.1	295.4	306.8	280.5	294.1	299.4	266.9	289.3	283.0	290.3	285.5	297.7	281.2	287.3	293.0	287.2
2.4	277.0	271.1	282.3	265.1	289.9	275.3	276.5	266.9	278.5	290.6	285.2	286.9	285.1	283.6	281.9	274.9	270.2
2.5	256.9	267.3	266.5	263.5	249.2	246.5	255.0	261.5	246.4	259.3	264.0	255.5	269.6	250.0	254.9	260.6	254.7
2.6	230.6	218.4	234.4	243.6	239.1	240.1	224.5	236.9	234.0	224.4	223.1	224.7	231.7	235.6	240.0	227.3	239.6
2.7	204.7	202.4	214.1	209.0	203.1	213.1	209.7	215.6	205.2	208.1	221.6	200.4	214.8	205.9	206.8	216.3	215.5
2.8	179.6	181.3	177.6	194.9	181.2	192.1	182.4	177.5	176.5	191.9	175.5	180.3	183.3	181.4	180.2	179.6	180.7
2.9	173.2	163.7	168.2	159.0	161.3	174.5	165.1	165.0	162.2	165.0	161.5	167.4	162.1	160.7	161.3	162.6	166.8
3	153.2	147.0	152.1	150.5	152.1	145.5	140.4	152.9	140.3	137.3	150.2	140.2	152.2	146.1	157.5	149.3	140.1
3.1	137.4	133.9	131.2	136.1	128.5	128.5	133.9	128.1	132.6	128.9	129.1	138.1	134.1	125.3	130.4	125.6	134.9
3.2	116.3	118.9	122.3	121.0	122.6	122.0	122.0	126.3	116.5	118.8	122.8	123.4	122.3	116.2	119.3	121.7	122.2
3.3	112.5	107.4	112.0	107.6	106.1	105.5	110.5	105.5	109.5	114.7	106.3	105.4	110.9	107.2	105.1	111.1	113.6
3.4	99.2	102.2	105.4	102.5	101.0	95.6	98.9	98.7	102.3	102.5	97.8	102.3	97.7	96.3	97.3	96.8	103.3
3.5	92.53	89.39	91.26	88.23	93.19	89.63	87.27	89.80	90.00	92.57	92.80	95.49	91.80	92.47	88.43	94.40	89.92
3.6	82.85	77.11	87.15	81.60	84.13	78.98	84.13	86.28	83.81	84.00	80.83	81.98	84.31	85.47	86.28	83.22	83.07
3.7	74.74	76.87	76.61	77.57	78.25	72.94	77.21	76.79	73.77	73.65	74.93	79.64	78.59	73.61	74.23	73.70	79.56
3.8	67.05	71.42	73.82	69.25	70.08	71.73	68.40	68.86	73.17	73.77	75.16	72.29	67.69	72.56	73.58	75.49	71.84
3.9	69.31	64.10	63.78	65.70	67.85	68.55	67.00	65.06	66.89	65.68	66.19	66.62	65.93	67.37	66.30	64.58	71.57
4	63.39	61.28	62.26	62.70	60.47	60.43	60.84	63.19	61.41	61.69	62.44	61.47	61.99	63.64	60.93	61.21	61.33
4.1	61.05	57.73	59.31	56.16	59.93	54.87	56.98	57.11	60.03	55.56	53.77	57.13	58.16	55.21	57.89	59.73	56.02
4.2	54.26	53.30	52.15	54.92	56.45	54.08	53.36	55.57	53.72	54.30	52.39	55.53	55.71	52.66	49.47	54.62	51.23
4.3	50.39	51.16	51.20	49.03	50.79	48.75	49.64	49.86	48.43	51.27	51.42	51.06	50.14	51.06	49.51	50.43	50.62
4.4	47.01	46.93	48.69	47.25	46.98	48.64	48.67	48.47	45.87	46.38	49.46	45.96	45.63	49.71	47.85	45.93	47.94
4.5	45.73	44.40	43.49	44.08	46.71	43.48	47.63	44.38	43.50	45.91	45.65	41.45	43.96	46.39	47.34	44.19	43.39
4.6	43.80	44.88	42.46	43.14	42.07	40.79	43.92	42.29	43.35	42.28	42.84	40.08	43.22	43.98	43.99	43.67	43.89
4.7	40.70	40.69	41.47	42.05	40.86	40.58	41.28	39.22	39.10	42.46	42.16	41.26	42.52	40.08	39.98	41.24	41.98

Time Step	Simulation Run Number															
	85	86	87	88	89	90	91	92	93	94	95	96	97	98	99	100
0.1	0.45	0.43	0.44	0.41	0.45	0.44	0.41	0.45	0.44	0.45	0.45	0.44	0.42	0.45	0.43	0.47
0.2	1.20	1.21	1.16	1.15	1.14	1.25	1.19	1.21	1.13	1.14	1.19	1.19	1.13	1.17	1.18	1.19
0.3	2.44	2.55	2.66	2.59	2.48	2.50	2.55	2.75	2.53	2.43	2.62	2.53	2.50	2.46	2.67	2.69
0.4	4.40	4.55	4.68	4.33	4.62	4.42	4.71	4.70	4.73	4.67	4.49	4.42	4.48	4.38	4.51	4.44
0.5	7.87	7.71	7.93	8.33	7.89	8.12	8.37	8.02	7.75	7.79	7.71	7.71	8.22	7.72	7.71	8.17
0.6	13.67	13.13	13.22	13.45	13.08	14.08	13.11	12.76	13.50	13.23	13.54	13.40	13.66	13.40	13.84	13.67
0.7	21.96	20.91	21.79	22.11	21.19	21.08	20.89	22.49	20.98	21.52	21.66	21.31	22.36	21.83	20.75	21.47
0.8	32.12	32.08	32.03	32.77	31.10	32.00	31.42	32.77	31.95	32.84	33.30	32.44	33.16	31.95	32.01	30.76
0.9	44.08	45.90	46.32	44.97	47.09	44.98	45.41	48.30	44.56	45.89	46.77	45.40	45.00	45.16	45.64	43.33
1	57.28	62.77	61.82	63.40	65.58	64.62	64.09	65.00	61.08	63.45	65.95	62.16	64.27	66.64	62.74	64.93
1.1	86.72	88.99	88.17	82.77	79.98	85.31	83.13	87.80	85.95	82.46	82.71	84.65	89.40	83.35	81.06	87.21
1.2	116.6	118.0	110.4	124.5	109.4	115.6	117.0	115.2	112.7	116.1	113.4	111.2	114.0	107.6	110.7	107.8
1.3	141.8	150.0	144.5	139.0	151.5	145.9	145.4	143.5	148.4	144.7	150.2	148.9	148.5	142.8	148.7	150.9
1.4	188.6	188.0	177.8	187.8	184.6	185.9	181.9	181.2	183.5	172.5	176.1	181.9	182.7	175.5	183.1	189.5
1.5	209.0	217.5	216.6	211.7	225.7	220.1	207.4	222.6	218.1	207.4	219.1	219.4	220.2	214.9	219.1	223.6
1.6	254.8	251.2	268.0	255.2	251.4	254.8	254.6	245.4	239.6	258.7	256.1	242.6	261.3	244.9	250.9	272.7
1.7	275.8	267.5	276.7	281.6	269.2	274.0	279.0	297.0	277.1	270.0	272.1	272.3	281.9	278.8	267.0	279.0
1.8	299.3	297.5	297.1	295.3	304.8	299.2	308.0	296.8	302.4	309.9	301.3	299.7	290.5	304.6	305.8	296.3
1.9	304.3	322.3	308.9	308.9	307.1	316.1	314.0	320.5	313.8	302.3	316.6	311.7	305.9	328.3	303.4	302.9
2	325.5	316.7	318.1	325.2	335.2	316.0	319.2	302.4	311.5	314.7	322.1	312.8	309.8	305.6	309.5	308.1
2.1	308.1	306.7	311.7	318.5	317.5	308.3	305.2	308.4	327.2	314.8	293.6	308.3	315.6	286.0	320.9	297.6
2.2	301.2	300.6	302.7	299.5	304.9	293.1	306.9	308.1	307.4	312.1	307.8	318.8	305.9	302.4	309.5	303.7
2.3	287.3	293.8	295.9	293.2	297.2	287.8	290.5	294.6	293.9	306.4	286.5	297.6	291.3	299.0	286.7	294.1
2.4	273.0	294.4	277.1	259.4	283.8	277.5	282.2	276.7	271.5	293.7	265.8	275.3	264.0	289.2	288.8	283.0
2.5	245.7	248.3	262.9	254.0	249.8	239.9	260.9	246.6	258.8	254.8	274.4	254.2	250.8	253.3	254.2	249.1
2.6	221.7	237.3	238.3	228.5	235.1	234.6	231.4	231.6	235.6	224.2	227.5	232.3	225.2	244.0	225.3	233.3
2.7	196.0	200.0	204.0	213.2	207.2	206.3	211.5	220.1	207.0	218.2	208.8	203.5	217.2	213.9	196.1	214.4
2.8	190.2	186.9	180.1	187.9	175.4	188.2	189.0	193.8	192.3	183.1	188.9	177.6	198.3	193.9	188.2	183.3
2.9	164.2	167.3	161.8	156.1	156.0	159.4	169.7	163.6	174.2	159.9	157.1	161.0	155.2	166.3	164.0	166.5
3	149.1	137.2	152.5	144.2	149.2	154.7	140.3	145.9	142.7	151.1	148.5	147.6	145.9	142.1	143.4	156.2
3.1	131.7	129.9	134.6	129.7	136.7	138.2	134.3	126.2	132.8	129.8	134.2	123.3	136.4	132.6	131.1	127.3
3.2	117.4	116.2	111.4	118.2	118.3	120.3	112.1	125.4	127.0	119.7	119.6	114.3	115.9	119.5	128.4	116.3
3.3	109.2	106.9	106.1	109.3	113.4	109.9	107.3	109.9	110.8	107.9	112.3	110.5	109.0	111.5	101.3	105.9
3.4	92.0	99.6	104.1	101.3	97.1	99.9	96.6	103.5	98.1	97.5	101.0	97.1	95.5	99.4	95.9	100.1
3.5	89.20	89.14	91.90	94.49	89.92	94.05	91.92	88.66	91.02	91.84	93.67	88.87	87.09	91.96	89.98	93.85
3.6	85.14	83.75	83.91	81.39	83.69	76.72	84.22	82.98	82.85	80.14	84.85	80.86	82.86	83.24	83.67	83.04
3.7	77.11	71.95	78.86	77.66	75.00	77.66	79.05	78.23	77.25	76.28	74.23	74.06	76.18	78.79	77.79	79.27
3.8	71.42	68.88	73.11	70.98	71.14	73.66	71.29	71.60	73.28	67.91	71.99	72.43	70.97	71.88	71.65	68.00
3.9	67.49	64.62	66.68	67.24	67.41	68.01	63.42	67.16	66.17	68.23	69.03	65.28	64.21	66.89	65.01	65.25
4	63.70	64.06	62.39	62.46	64.55	60.94	63.65	62.53	62.31	60.51	60.71	60.83	60.37	61.03	63.52	62.29
4.1	57.99	53.46	54.21	55.98	55.76	59.24	58.46	59.80	56.31	60.53	54.89	59.54	56.75	60.22	55.74	57.49
4.2	54.35	56.28	52.28	52.11	53.41	53.39	53.22	54.41	50.77	54.94	55.29	53.39	54.14	51.21	55.49	53.87
4.3	50.79	51.07	51.25	48.78	49.37	52.56	50.89	51.71	53.29	51.85	48.13	54.08	53.27	49.35	49.38	51.58
4.4	48.84	48.52	49.05	47.43	46.39	47.16	47.95	49.49	46.77	49.42	48.12	47.98	46.59	46.61	47.97	46.34
4.5	42.13	44.79	47.63	44.99	44.14	45.62	42.94	45.33	47.99	46.17	46.11	42.96	47.28	44.60	47.12	45.00
4.6	44.17	41.93	42.04	41.41	41.60	41.16	45.82	40.56	41.52	42.39	43.54	44.76	44.97	44.60	43.46	43.20
4.7	41.48	39.26	40.95	38.57	39.33	40.89	43.42	40.55	43.70	39.80	39.67	41.23	39.48	41.00	41.34	42.25

NO. OF COPIES ORGANIZATION

1 (PDF ONLY) DEFENSE TECHNICAL INFORMATION CTR
DTIC OCA
8725 JOHN J KINGMAN RD
STE 0944
FORT BELVOIR VA 22060-6218

1 US ARMY RSRCH DEV & ENGRG CMD
SYSTEMS OF SYSTEMS INTEGRATION
AMSRD SS T
6000 6TH ST STE 100
FORT BELVOIR VA 22060-5608

1 DIRECTOR
US ARMY RESEARCH LAB
IMNE ALC IMS
2800 POWDER MILL RD
ADELPHI MD 20783-1197

1 DIRECTOR
US ARMY RESEARCH LAB
AMSRD ARL CI OK TL
2800 POWDER MILL RD
ADELPHI MD 20783-1197

2 DIRECTOR
US ARMY RESEARCH LAB
AMSRD ARL CS OK T
2800 POWDER MILL RD
ADELPHI MD 20783-1197

1 AEROPREDICTION INC
ATTN F MOORE
9449 GROVER DRIVE, STE 201
KING GEORGE VA 22485

1 UNIV OF TEXAS AT ARLINGTON
MECH & AEROSPAC ENG DEPT
ATTN J C DUTTON
BOX 19018
500 W FIRST ST
ARLINGTON TX 76019-0018

2 ATK TACTICAL SYSTEMS DIV
ALLEGANY BALLISTICS LAB
ATTN D J LEWIS J S OWENS
210 STATE ROUTE 956
ROCKET CENTER WV 26726

1 ATK ADVANCED WEAPONS DIV
ATTN R H DOHRN
MN06-1000
5050 LINCOLN DR
EDINA MN 55436

NO. OF COPIES ORGANIZATION

1 ATK ORDNANCE SYS
ATTN B BECKER
MN07 MW44
505 LINCOLN DR
EDINA MN 55436

1 SCIENCE APPLICATIONS INTL CORP
ATTN J NORTHRUP
8500 NORMANDALE LAKE BLVD
SUITE 1610
BLOOMINGTON MN 55437

3 GOODRICH ACTUATION SYSTEMS
ATTN T KELLY P FRANZ
J CHRISTIANA
100 PANTON ROAD
VERGENNES VT 05491

2 ARROW TECH ASSOC
ATTN W HATHAWAY
MARK STEINOFF
1233 SHELBURNE RD STE D8
SOUTH BURLINGTON VT 05403

1 KLINE ENGINEERING CO INC
ATTN R W KLINE
27 FREDON GREENDEL RD
NEWTON NJ 07860-5213

1 GEORGIA INST TECH
DEPT AEROSPACE ENGR
ATTN M COSTELLO
270 FERST STREET
ATLANTA GA 30332

1 AIR FORCE RSRCH LAB
AFRL/MNAV
ATTN G ABATE
101 W EGLIN BLVD, STE 333
EGLIN AFB FL 32542-6810

1 COMMANDER
US ARMY ARDEC
AMSRD AAR AEM A
ATTN G MALEJKO
BLDG 95
PICATINNY ARSENAL NJ 07806-5000

1 COMMANDER
US ARMY ARDEC
ASMRD AAR AEP E
ATTN D CARLUCCI
BLDG 94
PICATINNY ARSENAL NJ 07806-5000

NO. OF
COPIES ORGANIZATION

1 COMMANDER
US ARMY ARDEC
ASMRD AAR AEP E
ATTN C KESSLER
BLDG 3022
PICATINNY ARSENAL NJ 07806-5000

1 COMMANDER
US ARMY ARDEC
ASMRD AAR AEP E
ATTN I MEHMEDAGIC
BLDG 94
PICATINNY ARSENAL NJ 07806-5000

1 PM MAS
ATTN SFAE AMO MAS
BLDG 354
PICATINNY ARSENAL NJ 07806-5000

3 US ARMY AMRDEC
AMSAM RD SS AT
ATTN R W KRETZSHMAR
L AUMAN E VAUGHN
REDSTONE ARSENAL AL 35898-5000

1 COMMANDER
US ARMY ARDEC
AMSTA DSA SA
ATTN A CLINE
BLDG 151
PICATINNY ARSENAL NJ 07806-5000

4 COMMANDER
US ARMY ARDEC
AMSRD AAR AEM I B 65N
ATTN J STEINER R P MAZESKI
D J DURKIN R MONTENEGRO
PICATINNY ARSENAL NJ 07806-5000

ABERDEEN PROVING GROUND

1 DIRECTOR
US ARMY RSCH LABORATORY
ATTN AMSRD ARL CI OK (TECH LIB)
BLDG 4600

14 DIRECTOR
US ARMY RSCH LABORATORY
ATTN AMSRD ARL WM J SMITH
AMSRD ARL WM B M ZOLTOSKI
AMSRD ARL WM BC P PLOSTINS
J NEWILL M CHEN (3 CYS)
J DESPIRITO J SAHU
B GUIDOS S SILTON
P WEINACHT M BUNDY